



## Structures of the tumor necrosis factor $\alpha$ inducing protein Tip $\alpha$ : A novel virulence factor from *Helicobacter pylori*

Tommaso Tosi<sup>1</sup>, Gianluca Cioci<sup>1</sup>, Karina Jouravleva, Cyril Dian, Laurent Terradot \*

European Synchrotron Radiation Facility, MX Group, BP 220, F-38043 Grenoble Cedex 9, France

### ARTICLE INFO

#### Article history:

Received 16 March 2009

Revised 8 April 2009

Accepted 20 April 2009

Available online 4 May 2009

Edited by Hans Eklund

#### Keywords:

Bacterial toxin

X-ray crystallography

Nucleus import

Inflammatory response

Stomach cancer

*Helicobacter pylori*

### ABSTRACT

*Helicobacter pylori* secretes a unique virulence factor, Tip $\alpha$ , that enters gastric cells and both stimulates the production of the TNF- $\alpha$  and activates the NF- $\kappa$ B pathway. The structures of a truncated version of Tip $\alpha$  (Tip $\alpha$ N34) in two crystal forms are presented here. Tip $\alpha$  adopts a novel  $\beta_1\alpha_1\alpha_2\beta_2\beta_3\alpha_3\alpha_4$  topology that can be described as a combination of three domains. A first region consists in a short flexible extension, a second displays a dodecin-like fold and a third is a helical bundle domain similar to the sterile alpha motif (SAM). Analysis of the oligomerisation states of Tip $\alpha$ N34 in the crystals and in solution suggests that the disulfide bridges could hold together Tip $\alpha$  monomers during their secretion in the gastric environment.

#### Structured summary:

MINT-7033680: TIP alpha (uniprotkb:B2UTN0) and TIP alpha (uniprotkb:B2UTN0) bind (MI:0407) by cosedimentation (MI:0027)

© 2009 Published by Elsevier B.V. on behalf of the Federation of European Biochemical Societies.

### 1. Introduction

*Helicobacter pylori* is a Gram-negative bacterium that colonises the human stomach. *H. pylori* is reported as the major cause of several gastric pathologies such as gastritis, peptic ulceration, stomach adenocarcinoma and mucosa-associated lymphoid tissue (MALT) lymphomas [1]. Virulence factors produced by *H. pylori* have a pivotal role in chronic inflammation and increase the risk of cancer [2,3]. The contribution of major virulence factors produced by *H. pylori* to cancer risks has been characterised such as the Cytotoxin associated gene A protein (CagA), the Vacuolating toxin A (VacA) and the BabA adhesin (reviewed in [2,4]). A highly immunogenic *H. pylori* protein, Tip $\alpha$  (for Tumor necrosis factor  $\alpha$  – TNF- $\alpha$  – inducing protein) was identified as a new virulence factor activating NF- $\kappa$ B and inducing the expression of TNF- $\alpha$ , a pro-inflammatory cytokine, produced in response to *H. pylori* infection [5–7]. Tip $\alpha$  also enhances the expression of different chemokines, upregulates Bcl-2 gene and downregulates p53 gene, thereby contribut-

ing to cancer establishment [8,9]. Tip $\alpha$  is present in all *H. pylori* genomes sequenced and has been detected in numerous clinical isolates from patients affected by gastritis, gastroduodenal ulcers and gastric cancers [6]. The mode of action of Tip $\alpha$  remains elusive but the protein has been shown to enter gastric cells and possibly penetrate the nucleus [10]. Tip $\alpha$  sequence displays no similarity to any known protein but a conserved motif has been proposed between Tip $\alpha$  and penicillin binding protein (PBP) suggesting that the protein might adopt a similar fold [11]. The protein is secreted in the extracellular medium [5,10,12,13] and forms homodimers of 38 kDa held together by inter-subunits disulfide bridges involving C25 and C27 [6]. *In vitro*, recombinant Tip $\alpha$  can bind both ss- and dsDNA [14]. A fragment of Tip $\alpha$  starting at residue 28 (delTip $\alpha$ ) showed a considerably reduced ability to induce TNF- $\alpha$  gene expression, NF- $\kappa$ B activation [6] and to enter gastric cells [10] suggesting an important role for the disulfide bridges.

We describe here the crystal structures of a truncated form of Tip $\alpha$  (Tip $\alpha$ N34) in two different crystal forms obtained at pH 4 and pH 8.5. These structures show that Tip $\alpha$  adopts a novel fold, consisting of an  $\alpha$ - $\beta$  sandwich combined with a helical bundle domain. Structural comparison and analysis provides insight into regions that may be involved in protein–protein interactions within the gastric cells. Gel filtration analysis of the oligomeric state of Tip $\alpha$  and Tip $\alpha$ N34 at different pHs suggests a role for the disulfide bridges during toxin secretion.

Abbreviations: MALT, mucosa-associated lymphoid tissue; PBP, penicillin binding protein; TEV, tobacco etch virus; SAD, single anomalous dispersion

\* Corresponding author.

E-mail address: [laurent.terradot@esrf.fr](mailto:laurent.terradot@esrf.fr) (L. Terradot).

<sup>1</sup> These authors contributed equally to this work.

## 2. Materials and methods

A DNA fragment corresponding to the secreted portion of Tip $\alpha$  (starting at M21) was amplified from *H. pylori* genomic DNA and cloned into pET151/D- topo vector (pET-Tip $\alpha$ ). The protein was expressed in *Escherichia coli* and purified with a His-trap column (GE Healthcare) equilibrated with buffer A (30 mM Tris pH 8, 200 mM NaCl, 5% glycerol). Tip $\alpha$  was eluted with a linear gradient of imidazole from 0 to 500 mM in Buffer A. After tobacco etch virus (TEV) cleavage, the protein was further purified by Nickel affinity and size-exclusion chromatography. Seleno-methionine incorporated Tip $\alpha$  (SeTip $\alpha$ ) was purified as Tip $\alpha$  except for NaCl concentration, raised to 500 mM in all buffers. Tip $\alpha$ N34 and SeTip $\alpha$ N34 were obtained by incubating respectively Tip $\alpha$  and SeTip $\alpha$  with trypsin at a protease/protein ratio of 1:1000 (w/w) on ice for 1 h. The vapour diffusion method was used for crystallisation. Form I crystals were grown by mixing equal amounts of protein (6 mg/ml) and reservoir solution containing 100 mM Na Citrate pH 4, 15 mM ATP and from 22% to 28% of Polyethylene glycol (PEG) 4000. Crystals of SeTip $\alpha$ N34 grew in 100 mM Na Citrate pH 4, 14% PEG6000 and 15 mM ATP. Crystal form II was obtained by mixing 2  $\mu$ l of Tip $\alpha$ N34 with 2  $\mu$ l of reservoir solution (100 mM Tris pH 8.5, 26% PEG4000, 50 mM MgCl<sub>2</sub>). Data were collected at ESRF beamlines (Table 1). Native and Se-Met crystal form I diffracted to 1.9 Å and 2.0 Å, respectively, and belonged to the space group *P2*<sub>1</sub> with two molecules per asymmetric unit (Table 1). A highly redundant dataset was collected at the Se edge with SeTip $\alpha$ N34 crystals. Se sites were used to obtain experimental phases using the single anomalous

dispersion (SAD) method followed by density modification using SHARP [15]. ARP-WARP [16] built an initial model that was completed manually and refined against the native data using REFMAC [17]. Crystal form II diffracted at 1.7 Å and belonged to the *P2*<sub>1</sub>*2*<sub>1</sub>*2*<sub>1</sub> space group with two molecules per asymmetric unit (Table 1). Crystal form II structure was solved by molecular replacement using PHASER [18] and the structure of form I as a search probe. The coordinates of Tip $\alpha$  crystal forms I and II structures have been deposited in the PDB, entry codes 2wcq and 2wcr, respectively. Analytical gel filtration experiments were performed by injecting 200  $\mu$ g of Tip $\alpha$  or Tip $\alpha$ N34 on a Superdex 75 10/300 column equilibrated in buffer A or in citrate buffer (50 mM citric acid pH 4, 200 mM NaCl). Details of the methods can be found in Supplementary data.

## 3. Results and discussion

### 3.1. Crystal structure of Tip $\alpha$ N34 form I

The structure of Tip $\alpha$ N34 monomer consists of an elongated, bean-shaped  $\alpha$ – $\beta$  sandwich combined to a helical bundle domain (Fig. 1A and B). It shows an original  $\beta_1\alpha_1\alpha_2\beta_2\beta_3\alpha_4$  topology completed by a short  $3_{10}$  helix at the N-terminal portion (Fig. 1A and B). The antiparallel  $\beta$ -sheet formed by  $\beta_1$ ,  $\beta_2$  and  $\beta_3$  wraps around the N-terminal half of  $\alpha_1$ . The C-terminal portion forms a four helix bundle with  $\alpha_2$ ,  $\alpha_3$  and  $\alpha_4$ , at the top of which lies a long loop connecting  $\alpha_1$ – $\alpha_2$  (Fig. 1B). Differences between the two subunits reside essentially at the N-terminal region, which appears more flexible with L37 to I52 displaying high B-factor values. This extension together with the bottom part of the  $\beta$ -sheet also mediates inter subunit contacts via hydrophobic interactions between V40, L45, Y42 and F139 from chain A with V40, M44, L45, F139 from chain B (Fig. 1C). Those contacts are reinforced by a network of hydrogen bonds between S58, H60, E137 from both subunits resulting in a head-to-head dimer related by a pseudo twofold axis (Fig. 1C and D). However, this dimer interface, burying 814 Å<sup>2</sup>, is centred on E137–E137 interactions, contacts that would likely be unfavoured in solution at a physiological pH.

### 3.2. Domain organisation and structural similarity with known proteins

A DALI [19] search identified more than 500 proteins with Z-scores lower than 4.3 but none of these structures were larger than 100 residues and no homologue was identified for the entire Tip $\alpha$ N34 structure. Structural homology analysis divides Tip $\alpha$ N34 in three parts: a N-terminal loop, consisting of residues N34 to I52, showing no similarities to existing structures. A second domain, consisting of  $\beta$ -strands  $\beta_1$ ,  $\beta_2$ ,  $\beta_3$  and the N-terminal half of  $\alpha_1$ , is similar to dodecin proteins, in particular to *H. salinarum* dodecin (pdb 1mog, rmsd 2.2 Å, 59 residues). Dodecins are small proteins that oligomerise in dodecamers and bind to FAD [20]. Tip $\alpha$ N34 superimposes well with dodecin monomer (Fig. 2A) but the FAD-binding residues (W36, E45 and Q55) are not conserved. The third domain consists of the helical bundle, similar to more than 100 proteins with best scores falling into three categories: (i) the nuclear abundant RNA-binding Nab2 protein (pdb 2v75, rmsd 2.7 Å, 70 residues), (ii) proteins containing the sterile alpha motif (SAM) domain and (iii) the translation initiation factor 2 alpha, aIF2 (pdb 1yz6, rmsd 4.8 Å, 90 residues) (Fig. 2B). The helical bundles of Tip $\alpha$  and Nab2 are similar to the PWI fold, a domain found in several nucleic acid binding proteins [21]. However, the motif involved in DNA binding in PWI-containing proteins is not conserved in Tip $\alpha$  nor in Nab2 [21]. More than 20 proteins containing a SAM domain were also identified as putative homologues, includ-

**Table 1**  
Data collection, phasing and refinement statistics.

	Tip- $\alpha$ N34 Se-Met pH 4	Tip- $\alpha$ N34 pH 4	Tip- $\alpha$ N34 pH 8.5
<b>Data collection statistics</b>			
Beamline	ID14-4	ID14-4	ID29
Unit cell (Å)			
a	31.64	31.36	48.88
b	102.21	101.99	67.26
c	47.53	47.25	97.47
$\beta$	94.40	94.38	
Space group	<i>P2</i> <sub>1</sub>	<i>P2</i> <sub>1</sub>	<i>P2</i> <sub>1</sub> <i>2</i> <sub>1</sub> <i>2</i> <sub>1</sub>
Wavelength (Å)	0.979	0.939	0.981
Resolution limit (Å)	43.0–2.0	50.9–1.9	27.7–1.7
Total observations	151 032 (22 287)*	93 609 (10 799)	128 160 (18 556)
Unique reflections	20 350 (2989)	22 965 (3030)	35 854 (5158)
Completeness	99.9 (99.9)	98.4 (90.4)	99.3 (99.6)
Multiplicity	7.4 (7.5)	4.1 (3.6)	3.6 (3.6)
$\langle I \rangle / \langle \sigma \rangle$	7.5 (1.8)	7.6 (2.2)	10.8 (1.9)
<i>R</i> <sub>merge</sub> (%) <sup>b</sup>	7.4 (40.3)	6.0 (32.5)	4.0 (40.7)
Wilson B-factor (Å <sup>2</sup> )	24.4	25.2	26.4
<b>Phasing statistics</b>			
Se sites	10		
FOM (centric/accentric)	0.13/0.41		
Anomalous phasing power	1.74		
<b>Refinement statistics</b>			
<i>R</i> <sub>cryst</sub>		19.6 (27.7)	18.2 (29.3)
<i>R</i> <sub>free</sub>		23.1 (37.7)	21.9 (34.7)
RMS bonds		0.015	0.017
RMS angles		1.482	1.51
Ramachandran outliers		Ile52B	Ser49A
<b>B-factors</b>			
Overall		28.0	17.0
Protein atoms		27.6	15.6
Water atoms		35.0	26.3

$$R_{\text{cryst}} = (\sum ||F_{\text{obs}} - F_{\text{calc}}||) / (\sum ||F_{\text{obs}}||).$$

\* Values in parentheses refer to the highest resolution shell.

$$^b R_{\text{merge}} = \sum ||I - \langle I \rangle|| / \sum \langle I \rangle.$$

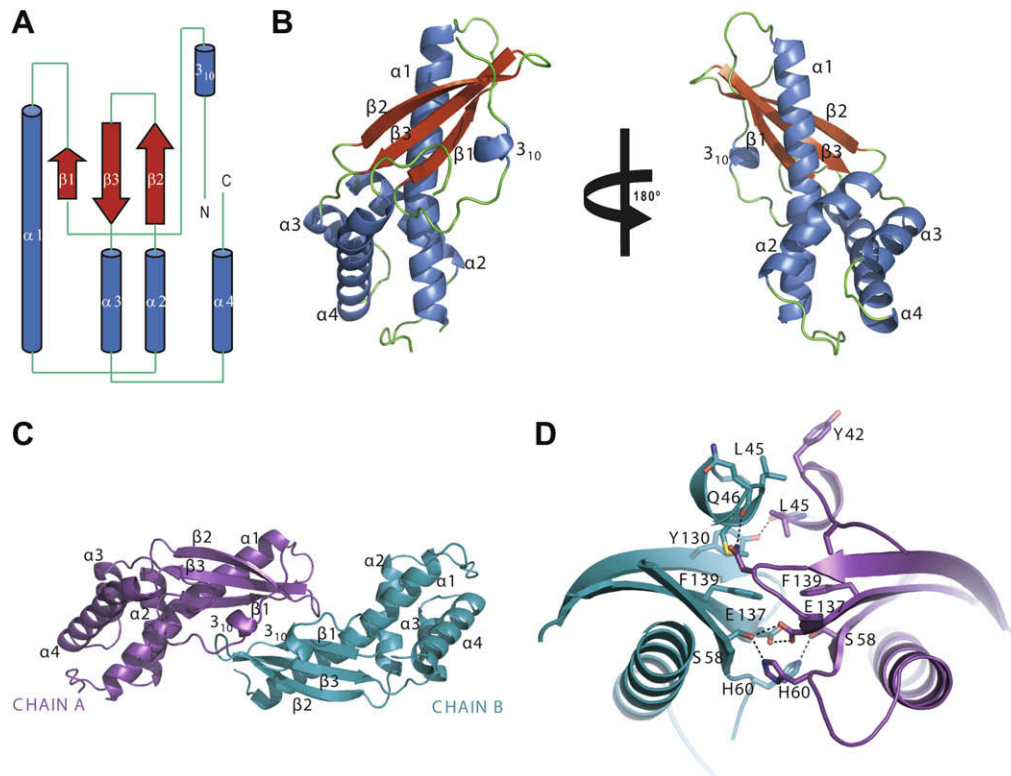


**Fig. 1.** Structure of Tip $\alpha$ N34. (A) Topology diagram of Tip $\alpha$ N34. (B) Two different views of Tip $\alpha$ N34 structure with  $\alpha$ -helices in blue,  $\beta$ -strands in red and loops in green. (C) Ribbon representation of the dimer with chain A and B colored in violet and blue, respectively. (D) Head-to-head dimer interface depicted in ribbon with side chains indicated as sticks (with carbon atoms colored depending of the subunit, nitrogen in blue, oxygen in red and sulfur in yellow).

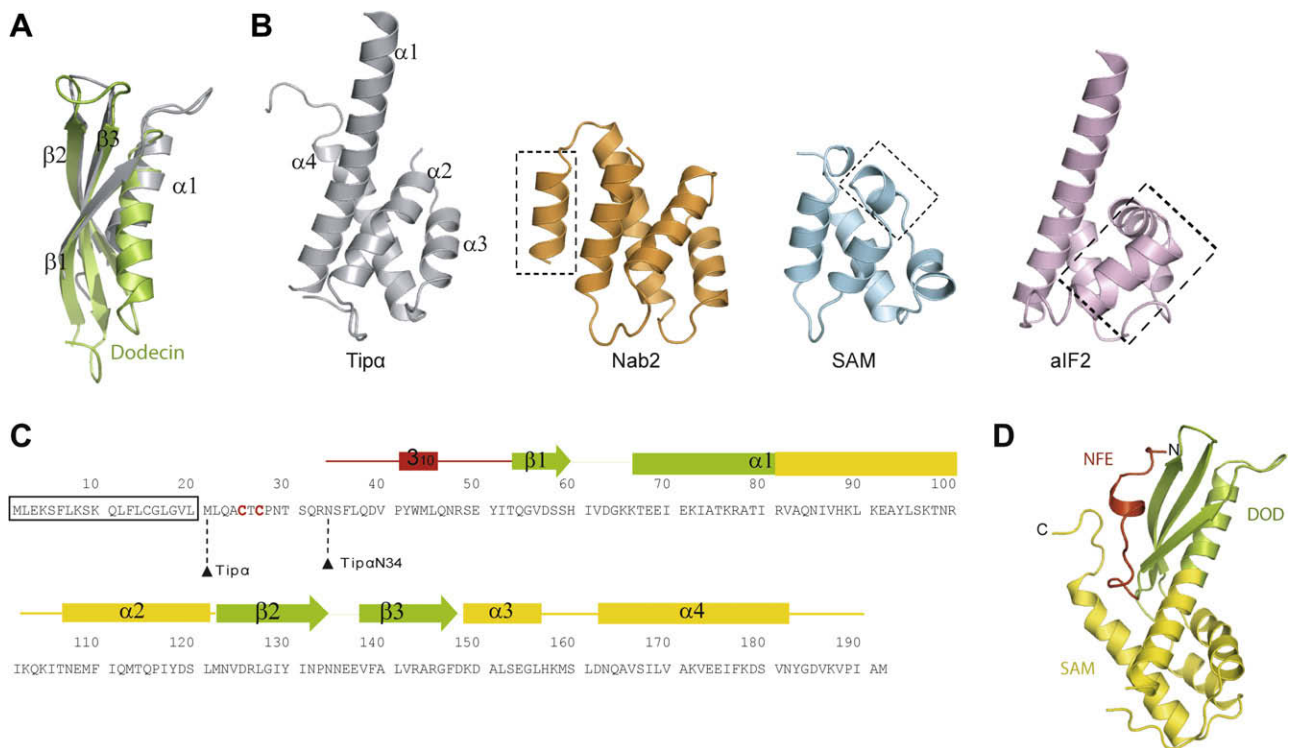


**Fig. 2.** Domain organisation of Tip $\alpha$  structure. (A) Structural superimposition of Tip $\alpha$ N34 DOD (grey) with dodecin (green). (B) Comparison of the Tip $\alpha$  SAM domain (grey) with the structure of Nab2 (orange), SAM domain from polyhomeotic-proximal chromatin protein (blue) and aIF2 (pink). Areas of main divergence are indicated by dashed boxes. (C) Sequence of Tip $\alpha$  with secondary structures indicated above and colored according to their respective domains (NFE, red; DOD, green and SAM, yellow). The signal peptide is indicated by a black box, C25 and C27 are colored in red. Starting residues for Tip $\alpha$  and Tip $\alpha$ N34 are indicated. (D) Structure of Tip $\alpha$ N34 colored according to domain boundaries.

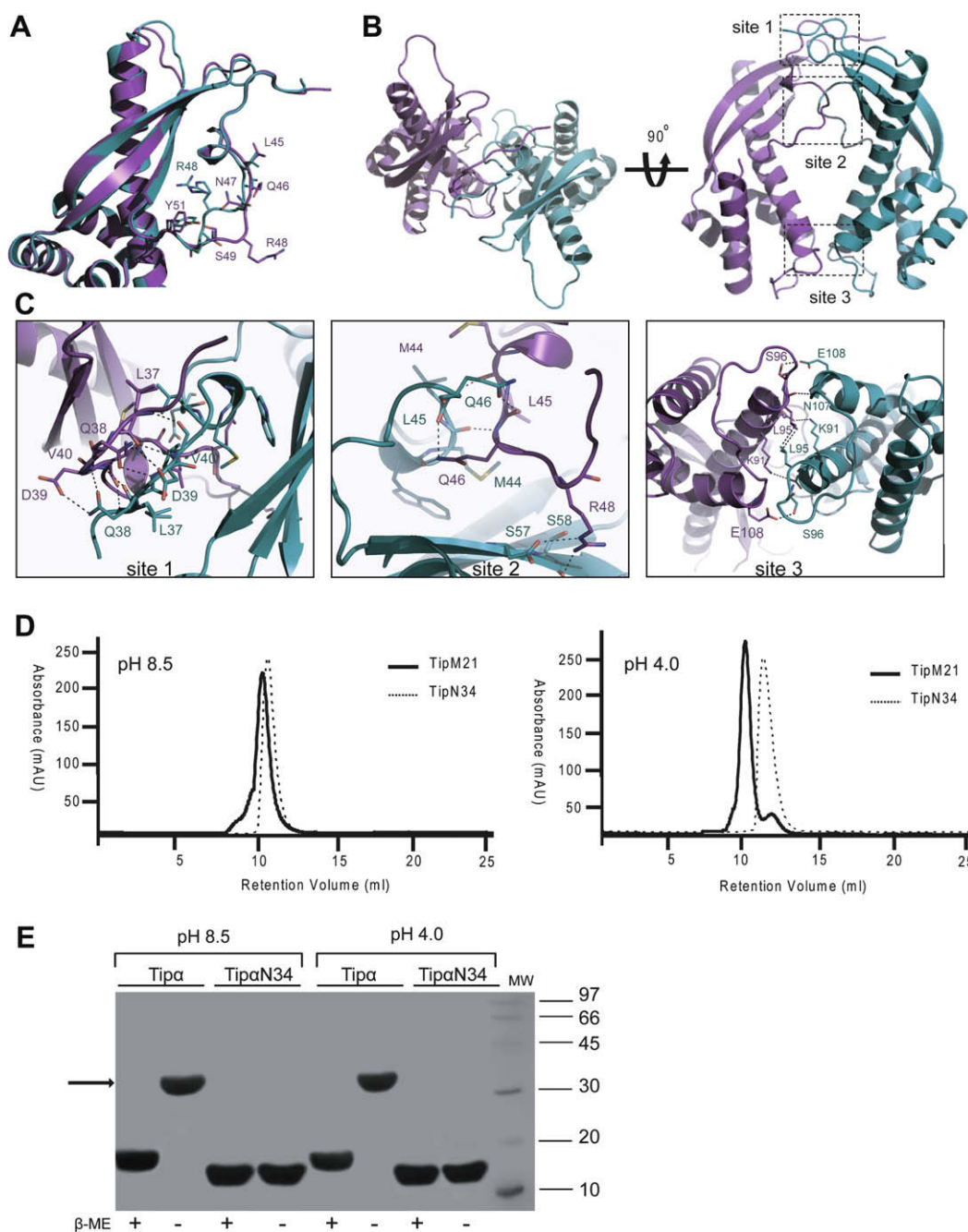


**Fig. 3.** Crystal form II of TipαN34. (A) Superimposition of chain A and chain B showing the different conformations of NFE loop. (B) Two views of the dimer of TipαN34 at pH 8.5 with chain A and B colored in violet and blue, respectively. Dotted boxes point to the three contact sites between subunits. (C) Close-up view of TipαN34 dimer interaction sites indicated in (A). Side chains of the residues involved are displayed in sticks. (D) Gel filtration analysis of Tipα and TipαN34 at pH 4 and pH 8.5. (E) SDS-PAGE analysis of the gel filtration experiments at pH 8.5 and pH 4 in the presence or absence of 5 mM β-mercapto-ethanol (β-ME). The arrow indicates Tipα dimer and the molecular weight markers (MW) sizes are indicated on the right in kDa.

ing polyhomeotic-proximal chromatin, sex comb, aveugle and ephA4 receptor tyrosine kinase. SAM domains are short domains found in a wide variety of eukaryotic proteins and in few bacterial ones [21,22]. The structural similarity of Tipα to SAM domain raises interesting questions since these domains can mediate protein–protein, protein–DNA and protein–RNA interactions [23]. TipαN34 also resembles domain II of aIF2 (archaea) and eIF2 (eukaryotes) but with a high rmsd and a good fit only with α1 (Fig. 2D). Thus, the structure of TipαN34 can be considered as a novel fold containing three regions: a N-terminal flexible extension (NFE), a dodecin-like domain (DOD) and a SAM-like domain (SAM) (Fig. 2C and D).

### 3.3. Crystal structure of form II and dimer organisation

The structure of crystal form II monomer is essentially identical to crystal form I. Major differences are located in the NFE region that undergoes an important conformational change that swaps the orientation of the N-terminus. Strand β<sub>1</sub> is rotated by 45° and both β<sub>2</sub> and β<sub>3</sub> are shifted in the structure at pH 4 compared to the crystal form I. Noteworthy, this extension adopts very different conformations in the two chains (Fig. 3A). In chain A, residues from this loop have their side chains oriented towards the solvent, disconnecting the loop from the rest of the molecule and forming a small solvent channel (Fig. 3A). In chain B, the same side chains,



in particular R48, point towards the concave face of the protein which changes the orientation of the loop and closes the solvent channel. The two molecules in the asymmetric unit are arranged in a different dimer than form I (Figs. 1D and 3B). This arrangement also generates a pseudo twofold symmetry axis that goes from the distal N-terminus to the helical bundle burying a total of 1358 Å<sup>2</sup> (Fig. 3B). The two subunits are held together by numerous electrostatic and few hydrophobic interactions in three sites (Fig. 3C). At site 1 the NFEs interact with each other. L37, Q38, D39 and V40 of chain A interact with V40, D39, Q38 and L37 of Chain B, respectively, to form a highly connected structure (Fig. 3C). At site 2, the NFEs interact with each other and the NFE from chain A also contacts β1 of chain B. NFEs interactions include hydrogen bonds between M44 and Q46 and L45 and Q46. In addition, Q46A side chain interacts also with W43 of chain B. On one side only, the side chain of R38 from chain A interacts with D57 from chain B (Fig. 3C). Site 3 comprises interactions between K91 and E92, L95 and N107, S96 and E108, and L95 side chains from both chains.

### 3.4. Oligomeric state of Tipα

To determine the oligomerisation states of Tipα and TipαN34 in solution, we performed analytical gel filtration experiments (Fig. 3D). At pH 8.5, both Tipα and TipαN34 eluted at a retention volume of 10.9 ml, corresponding to a molecular weight of around 30 kDa, in agreement with a theoretical Tipα homodimer. To mimic the form I crystallisation conditions, we performed analytical gel filtrations at pH 4 and found that TipαN34 eluted at 12 ml, corresponding to a monomer. In contrast, Tipα still eluted as a dimer at around 10.9 ml (Fig. 3D). SDS–PAGE experiments on protein samples corresponding to the elution peak of the two gel filtration experiments, confirm that, in absence of reducing agent, Tipα forms dimers but not TipαN34 (Fig. 3E). This strongly suggests that crystal form I dimer is likely a crystallisation artefact and that TipαN34 dimer observed in crystal from II at pH 8.5 is more likely to be relevant in solution.

## 4. Conclusions

Tipα is a unique virulence factor, secreted by all *H. pylori* strains, capable of penetrating gastric cells [10]. Our study reveals that this protein adopts an original fold with no resemblance to known PBPs as previously suggested. Tipα structure is a combination of three interconnected regions. These domains point towards putative protein–protein or protein–nucleic acid interaction sites that could play important roles in Tipα function. Finally, C25 and C27 were suggested to be crucial for dimer formation and Tipα activity [10,14]. We have shown that the two cysteines C25 and C27 are not necessary for Tipα to form a dimer at pH 8.5. However, at pH 4, their presence seems to be required in solution to hold the two subunits together. It is possible that *in vivo* these disulfide bridges could be necessary for keeping Tipα in its dimeric form when released into the acidic extracellular medium, i.e., the gastric mucosa.

## Acknowledgements

We wish to thank members of the MX group at ESRF for help during data collection and Joanna Timmins for critical comments

on the manuscript. This work was funded by the ESRF “In House Research” program.

## Appendix A. Supplementary data

Supplementary data associated with this article can be found, in the online version, at doi:10.1016/j.febslet.2009.04.033.

## References

- [1] IARC (1994) Schistosomes, liver flukes and *Helicobacter pylori*. IARC Working Group on the evaluation of carcinogenic risks to humans. Lyon, 7–14 June 1994. IARC Monogr. Eval. Carcinog. Risks Hum. 61, 1–241.
- [2] Franco, A.T. et al. (2008) Regulation of gastric carcinogenesis by *Helicobacter pylori* virulence factors. Cancer Res. 68, 379–387.
- [3] Ferreira, A.C., Isomoto, H., Moriyama, M., Fujioka, T., Machado, J.C. and Yamaoka, Y. (2008) *Helicobacter* and gastric malignancies. Helicobacter 13 (Suppl. 1), 28–34.
- [4] McNamara, D. and El-Omar, E. (2008) *Helicobacter pylori* infection and the pathogenesis of gastric cancer: a paradigm for host–bacterial interactions. Dig. Liver Dis. 40, 504–509.
- [5] Yoshida, M. et al. (1999) Cloning and characterization of a novel membrane-associated antigenic protein of *Helicobacter pylori*. Infect. Immun. 67, 286–293.
- [6] Suganuma, M., Kurusu, M., Suzuki, K., Nishizono, A., Murakami, K., Fujioka, T. and Fujiki, H. (2005) New tumor necrosis factor-α-inducing protein released from *Helicobacter pylori* for gastric cancer progression. J. Cancer Res. Clin. Oncol. 131, 305–313.
- [7] Suganuma, M., Kurusu, M., Okabe, S., Sueoka, N., Yoshida, M., Wakatsuki, Y. and Fujiki, H. (2001) *Helicobacter pylori* membrane protein 1: a new carcinogenic factor of *Helicobacter pylori*. Cancer Res. 61, 6356–6359.
- [8] Cheng, P., Shi, R.H., Zhang, H.J., Yu, L.Z., Zhang, G.X. and Hao, B. (2008) Effects of tumor necrosis factor-α inducing protein-α secreted by *Helicobacter pylori* on human gastric epithelial cells. Zhonghua Yi Xue Za Zhi 88, 1528–1532.
- [9] Kuzuhara, T., Suganuma, M., Kurusu, M. and Fujiki, H. (2007) *Helicobacter pylori*-secreting protein Tipα is a potent inducer of chemokine gene expressions in stomach cancer cells. J. Cancer Res. Clin. Oncol. 133, 287–296.
- [10] Suganuma, M. et al. (2008) TNF-α-inducing protein, a carcinogenic factor secreted from *H. pylori*, enters gastric cancer cells. Int. J. Cancer 123, 117–122.
- [11] Kuzuhara, T., Suganuma, M., Tsuge, H. and Fujiki, H. (2005) Presence of a motif conserved between *Helicobacter pylori* TNF-α inducing protein (Tipα) and penicillin-binding proteins. Biol. Pharm. Bull. 28, 2133–2137.
- [12] Godlewska, R., Pawlowski, M., Dzwonek, A., Mikula, M., Ostrowski, J., Dreła, N. and Jagusztyn-Krynicka, E.K. (2008) Tip-α (hp0596 gene product) is a highly immunogenic *Helicobacter pylori* protein involved in colonization of mouse gastric mucosa. Curr. Microbiol. 56, 279–286.
- [13] Suganuma, M., Kuzuhara, T., Yamaguchi, K. and Fujiki, H. (2006) Carcinogenic role of tumor necrosis factor-α inducing protein of *Helicobacter pylori* in human stomach. J. Biochem. Mol. Biol. 39, 1–8.
- [14] Kuzuhara, T., Suganuma, M., Oka, K. and Fujiki, H. (2007) DNA-binding activity of TNF-α inducing protein from *Helicobacter pylori*. Biochem. Biophys. Res. Commun. 362, 805–810.
- [15] de La Fortelle, E. and Bricogne, G. (1997) Maximum-likelihood heavy-atom parameter refinement in the MIR and MAD methods.
- [16] Perrakis, A., Morris, R. and Lamzin, V.S. (1999) Automated protein model building combined with iterative structure refinement. Nat. Struct. Biol. 6, 458–463.
- [17] Murshudov, G.N., Vagin, A.A., Lebedev, A., Wilson, K.S. and Dodson, E.J. (1999) Efficient anisotropic refinement of macromolecular structures using FFT. Acta Crystallogr. D Biol. Crystallogr. 55, 247–255.
- [18] McCoy, A.J., Grosse-Kunstleve, R.W., Adams, P.D., Winn, M.D., Storoni, L.C. and Read, R.J. (2007) Phaser crystallographic software. J. Appl. Crystallogr. 40, 658–674.
- [19] Holm, L. and Sander, C. (1998) Dictionary of recurrent domains in protein structures. Proteins 33, 88–96.
- [20] Grininger, M., Seiler, F., Zeth, K. and Oesterhelt, D. (2006) Dodecin sequesters FAD in closed conformation from the aqueous solution. J. Mol. Biol. 364, 561–566.
- [21] Grant, R.P. et al. (2008) Structure of the N-terminal Mlp1-binding domain of the *Saccharomyces cerevisiae* mRNA-binding protein, Nab2. J. Mol. Biol. 376, 1048–1059.
- [22] Ponting, C.P. (1995) SAM: a novel motif in yeast sterile and *Drosophila* polyhomeotic proteins. Protein Sci. 4, 1928–1930.
- [23] Kim, C.A. and Bowie, J.U. (2003) SAM domains: uniform structure, diversity of function. Trends Biochem. Sci. 28, 625–628.